Acta Neuropathol (2010) 120:195–207
DOI 10.1007/s00401-010-0685-y

ORIGINAL PAPER

Distinct glutaminyl cyclase expression in Edinger–Westphal nucleus, locus coeruleus and nucleus basalis Meynert contributes to pGlu-Aβ pathology in Alzheimer's disease

Markus Morawski · Maike Hartlage-Rübsamen · Carsten Jäger · Alexander Waniek · Stephan Schilling · Claudia Schwab · Patrick L. McGeer · Thomas Arendt · Hans-Ulrich Demuth · Steffen Roßner

Received: 20 January 2010 / Revised: 31 March 2010 / Accepted: 2 April 2010 / Published online: 10 April 2010
© The Author(s) 2010. This article is published with open access at Springerlink.com

Abstract Glutaminyl cyclase (QC) was discovered recently as the enzyme catalyzing the pyroglutamate (pGlu or pE) modification of N-terminally truncated Alzheimer's disease (AD) Aβ peptides in vivo. This modification confers resistance to proteolysis, rapid aggregation and neurotoxicity and can be prevented by QC inhibitors in vitro and in vivo, as shown in transgenic animal models. However, in mouse brain QC is only expressed by a relatively low proportion of neurons in most neocortical and hippocampal subregions. Here, we demonstrate that QC is highly abundant in subcortical brain nuclei severely affected in AD. In particular, QC is expressed by virtually all urocortin-1-positive, but not by cholinergic neurons of the Edinger–Westphal nucleus, by noradrenergic locus coeruleus and by cholinergic nucleus basalis magnocellularis neurons in mouse brain. In human brain, QC is expressed by both, urocortin-1 and cholinergic Edinger–Westphal neurons and by locus coeruleus and nucleus basalis Meynert neurons. In brains from AD patients, these neuronal populations displayed intraneuronal pE-Aβ immunoreactivity and morphological signs of degeneration as well as extracellular pE-Aβ deposits. Adjacent AD brain structures lacking QC expression and brains from control subjects were devoid of such aggregates. This is the first demonstration of QC expression and pE-Aβ formation in subcortical brain regions affected in AD. Our results may explain the high vulnerability of defined subcortical neuronal populations and their central target areas in AD as a consequence of QC expression and pE-Aβ formation.

Keywords Alzheimer's disease · Locus coeruleus · Edinger–Westphal nucleus · Nucleus basalis Meynert · Glutaminyl cyclase · Pyroglutamate-Abeta

M. Morawski and M. Hartlage-Rübsamen contributed equally to this manuscript.

M. Morawski · M. Hartlage-Rübsamen · C. Jäger · A. Waniek · T. Arendt · S. Roßner (✉)
Paul Flechsig Institute for Brain Research, University of Leipzig, Jahnallee 59, 04109 Leipzig, Germany
e-mail: steffen.rossner@medizin.uni-leipzig.de

S. Schilling · H.-U. Demuth
Probiodrug AG, Weinbergweg 22, Biocenter, 06120 Halle/Saale, Germany

C. Schwab · P. L. McGeer
Kinsmen Laboratory of Neurological Research, Department of Psychiatry, University of British Columbia, Vancouver, BC, Canada

H.-U. Demuth
Ingenium Pharmaceuticals GmbH, Fraunhoferstr. 13, 82152 Martinsried/Munich, Germany

Abbreviations

AD	Alzheimer's disease
APP	Amyloid precursor protein
CBF	Cholinergic basal forebrain
ChAT	Choline acetyltransferase
CRF	Corticotropin-releasing factor
DAB	3,3′-Diaminobenzidine
EWN	Edinger–Westphal nucleus
LC	Locus coeruleus
Nbm	Mouse nucleus basalis magnocellularis
NbM	Human nucleus basalis Meynert
pE-Aβ	Pyroglutamate-modified Aβ
QC	Glutaminyl cyclase
TH	Tyrosine hydroxylase
Ucn-1	Urocortin-1

Introduction

The appearance of neurofibrillary tangles, loss of specific neuronal populations and deposits of Aβ peptides in neocortical brain structures are major histopathological hallmarks of Alzheimer's disease (AD) [60]. Aβ peptides are liberated from the amyloid precursor protein (APP) after sequential enzymatic action of β- and γ-secretases. The γ-secretase cleavage results in the generation of $Aβ_{1–40}$ and $Aβ_{1–42}$ peptides, which exhibit different potencies of aggregation, fibril formation and neurotoxicity [17, 23, 24, 44, 62]. Additionally, N-terminally truncated Aβ peptides displaying an N-terminal glutamate residue are abundant in brains from AD patients [29, 46, 51, 61, 64]. A substantial proportion of these N-truncated Aβ peptides undergoes subsequent cyclization of N-terminal glutamate (E) into pyroglutamate (pE) [50, 51]. The resulting pE-Aβ peptides have been shown to be a major constituent of Aβ deposits in sporadic and familial AD [38, 43, 50, 73]. Thus, the assumption has been made that pE-Aβ peptides could play a prominent role in AD pathogenesis.

This view is supported by a number of experimental observations. For example, a particular neurotoxicity of pE-Aβ peptides in primary neurons, neuronal cell lines and transgenic animals has been demonstrated [1, 47, 72]. Moreover, pE-modification of N-truncated Aβ peptides is believed to have a significant influence on plaque generation and clearance. So it has been shown that the cyclization of glutamate into pE leads to a loss of N-terminal charge resulting in accelerated aggregation of pE-Aβ when compared with unmodified Aβ peptides [19, 47] and that pE-Aβ acts as a seed for aggregation as well as for co-aggregation of non-modified Aβ peptides [12, 36, 53, 56]. Furthermore, cyclization of N-terminal glutamate of Aβ peptides confers resistance to degradation by most aminopeptidases as well as Aβ-degrading endopeptidases [49].

However, for a long time, the molecular pathway leading to N-terminal glutamate cyclization of truncated Aβ peptides remained elusive. Recently, glutaminyl cyclase (QC) has been shown to be the enzyme catalyzing pE-Aβ peptide generation in vitro [52] and in vivo [11, 54, 55]. Chronic inhibition of QC in transgenic mouse models of AD resulted in reduced pE-Aβ peptide generation and in diminished total Aβ peptide concentrations [54]. Thus, the enzymatic activity of QC appears to be a prerequisite for pE-Aβ peptide generation and, therefore, QC-expressing neurons may be at special risk for degeneration. In a recent study focussing on QC expression in telencephalic and diencephalic mouse brain regions, we observed QC in a subpopulation of lateral and paraventricular hypothalamic neurons and in a moderate number of GABAergic interneurons in the hippocampal molecular layer, in the hilus of the dentate gyrus and in all layers of the neocortex [18]. However, the proportion of QC neurons in cortex and hippocampus displaying pronounced immunoreactivity was rather low (0.5–2%), which may explain the lack of substantial neurodegeneration in these brain structures in APP transgenic mouse models. On the other hand, even the degeneration of a small number of GABAergic interneurons in the hippocampus may have perturbing effects on long-term potentiation and on the performance in learning/memory tests [66].

In AD, in addition to neocortical and hippocampal neurodegeneration and Aβ plaque pathology, there is a selective loss of defined neuronal populations in distinct subcortical brain nuclei, including the nucleus basalis Meynert (NbM) of the cholinergic basal forebrain [2, 9, 70], the Edinger–Westphal nucleus (EWN) [21, 45, 58, 59] and the locus coeruleus (LC) [5, 6, 16, 32, 67]. Therefore, we asked whether QC may be expressed by neurons of these nuclei and, if so, whether it may contribute to pE-Aβ pathology.

Materials and methods

Experimental animals

Wild type C57Bl6 mice and QC knock-out mice aged 2–3 months ($N = 4$ each) were used for the immunohistochemical analysis of QC expression in EWN, LC and Nbm. QC knock-out mice were generated on the basis of a classical homologous recombination approach. Cre-mediated excision of exons 5 and 6 was confirmed by PCR and RT-PCR. The constitutive deletion of these exons resulted in an additional frame shift and thus in a complete loss of the C-terminal part of the protein (not shown).

Preparation of mouse brain samples for immunohistochemistry

Mice were anaesthetised with pentobarbital and perfused transcardially with 25 ml phosphate-buffered saline (PBS 0.01 M, pH 7.4) followed by perfusion with 25 ml 4% paraformaldehyde in phosphate buffer (PB 0.1 M, pH 7.4). The brains were removed from the skull and postfixed by immersion in the same fixative overnight at 4°C. After cryoprotection in 30% sucrose in 0.1 M PB for 3 days, the brains were snap-frozen in *n*-hexane at −68°C and stored at −20°C. Coronal sections (30 µm) were cut on a sliding microtome and collected in 0.1 M PB.

Human brain tissue

Tissue preparation

Fifteen mm-thick tissue blocks were prepared in the frontal plane according to the atlas of the human brain [31] and fixed in 4% paraformaldehyde for 3–4 days. Areas containing the regions of interest were cryoprotected in 30% sucrose in 0.1 M PBS, pH 7.4. Series of 30 µm-thick sections were cut on a freezing microtome and collected in PBS containing 0.1% sodium azide.

Identification of anatomical regions and applied nomenclature

Anatomical regions were identified using Nissl-stained sections and the atlas of the human brain [31]. The nomenclature of brain regions was mainly adopted from atlases of human brain [31], human brainstem [42] and rhesus monkey brain [41]. We additionally used the data of detailed anatomical descriptions of the EWN [21, 22], the LC [33, 34] and the NbM [2].

Characterization of human brain tissue

The EWN, LC and NbM were evaluated for QC expression and for pE-Aβ deposition in brains from eight AD cases and from eight age-matched control subjects (Table 1). The definite diagnosis of AD for all cases used in this study was based on the presence of neurofibrillary tangles and neuritic plaques in the hippocampal formation and neocortical areas and met the criteria of the National Institute of Neurologic and Communicative Disorders and Stroke and the Alzheimer's Disease and Related Disorders Association [37]. Brain tissue containing the EWN (Talairach space 28–29 mm) according to [31], the LC (Obex 20–32) according to [42] and the NbM (Ch4; Talairach space −2 to −0.6 mm) according to [2, 31] from the same cases was used for immunohistochemistry to detect the presence of QC, pE-Aβ and neuronal markers. Case recruitment and autopsy were performed in accordance with guidelines set by the Ethical Committees of the University of British Columbia and the Leipzig University (License# 063/2000). The required consent was obtained for all cases.

Immunohistochemistry for QC, Ucn-1, ChAT, TH and pE-Aβ

All immunohistochemical procedures were performed on free-floating brain sections. Immunohistochemistry in human brain to detect QC was performed using the rabbit antiserum 1301 (1:500), which was raised against recombinant full length mouse QC expressed in yeast.

The polyclonal antiserum was purified using a HiTrap rProtein A FF prepacked column (5 ml, GE Healthcare) and antibody elution by a shift to pH 3 using a citric acid buffer. The neutralised protein solution was stored at −20°C after addition of 50% glycerol. The antibody showed no significant differences in detecting mouse, rat and human QC in western blot analysis and immunohistochemistry, which appears conceivable considering a 85% protein sequence identity. Moreover, the specificity of the QC antiserum was previously shown by the robust labelling of mouse hypothalamic neurons, a known source of QC and of peptide hormones modified by QC, and by the absence of this labelling in brains from QC knock-out mice [18]. Additionally, the specificity of QC immunolabelling was validated by similar staining patterns obtained using a commercially available mouse anti-human QC antiserum (Abnova 1:500). On consecutive human brain sections, the neuronal markers urocortin-1 (Ucn-1), choline acetyltransferase (ChAT) and tyrosine hydroxylase (TH) as well as pE-Aβ were detected using the following antisera: goat anti-Ucn-1 (St. Cruz 1:200), goat anti-ChAT (Millipore 1:500), mouse anti-TH (Millipore 1:500) and mouse anti-pE-Aβ (Synaptic Systems 1:200). All sections were pretreated with an initial antigen retrieval step by heating to 90°C in 0.1 M citrate buffer, pH 2.5, for 3 min followed by rinsing with PBS-T. Brain sections were further treated with 60% methanol, 2% H_2O_2 for 1 h prior to incubation with the primary antibodies at 4°C overnight in a humid chamber. The following day sections were incubated with secondary biotinylated donkey anti-rabbit, donkey anti-mouse or donkey anti-goat antibodies (Dianova 1:1,000) for 60 min at room temperature followed by the ABC method, which comprised incubation with complexed streptavidin—biotinylated horseradish peroxidase. Incubations were separated by washing steps (3 times 5 min in PBS-T). Binding of peroxidase was visualised by incubation with 2 mg 3,3′-diaminobenzidine (DAB), 20 mg nickel ammonium sulphate and 2.5 µl H_2O_2 per 5 ml Tris buffer (0.05 M, pH 8.0) for 1–2 min. The enzymatic reaction resulted in black labelling, which was well distinguishable from the brown neuropigment present in many human LC neurons.

Immunohistochemistry in brains from wild type and QC knock-out mice was performed similarly but developed by incubation with 4 mg DAB and 2.5 µl H_2O_2 per 5 ml Tris buffer (0.05 M, pH 7.6) for 1–2 min resulting in a brown reaction product [18]. In control experiments, primary antibodies were omitted, resulting in absence of staining.

Double immunofluorescent labelling procedures

In order to relate QC expression in mouse brain to marker proteins of defined neuronal populations, double

Table 1 Human brain tissue used for QC and pE-Aβ labellings

Case #	PMD (h)	Gender	Age (years)	Brain weight (g)	COD	Braak staging
Control						
1	48	Female	75	1,130	Cardial infarction	0
2	72	Female	68	1,284	Bronchopneumonia	0
3	24	Female	82	1,180	Ovarian cancer	0
4	48	Male	78	1,420	Cardial infarction	0
5	9	Female	43	n.a.	Drug overd. (insulin)	0
6	24	Female	80	1,190	Lung cancer	0
7	25	Female	75	1,234	Lung cancer	0
8	7	Male	78	1,394	Pulmonary failure	0
Mean	32.1	6/2	72.4			
AD						
1	55	Female	95	1,060	Cardial infarction	VI
2	32	Female	70	1,200	Respiratory failure	IV
3	28	Male	68	960	Bronchopneumonia	VI
4	6	Female	58	1,010	Respiratory failure	IV
5	16	Female	65	1,080	Respiratory failure	V
6	40	Female	79	1,006	n.a.	IV
7	24	Male	69	934	n.a.	V
8	42	Female	91	1,230	Stroke	IV
Mean	30.4	6/2	74.4			

AD Alzheimer's disease, *PMD* postmortem delay, *COD* cause of death, *EC* entorhinal cortex

immunofluorescent labellings were performed using rabbit anti-QC antiserum 1301 (1:250) combined with goat anti-Ucn-1 (1:100), goat anti-ChAT (1:250) and mouse anti-TH (1:250), respectively. Brain sections were incubated with cocktails of primary antibodies overnight at 4°C. The following day, sections were washed three times with TBS and were then incubated with appropriate cocktails of secondary antibodies (i.e. biotinylated donkey or goat anti-rabbit; 1:400 and Cy3-conjugated goat anti-mouse or donkey anti-goat, 1:200 Dianova) for 60 min at room temperature. After washing, brain sections were incubated with streptavidin-Cy2 conjugates (Dianova 1:100) for 45 min, washed again and mounted onto gelatine-coated slides. In double immunofluorescent labellings, the omission of one primary antibody resulted in the depletion of the corresponding fluorescent signal without affecting the detection of the second antigen.

Microscopy

Light microscopy

Tissue sections were examined with a Zeiss Axiovert 200 M microscope equipped with a motorised stage (Märzhäuser, Germany) with MosaiX software and by means of a CCD camera (Zeiss MRC) connected to an Axiovision 4.6 image analysis system (Zeiss, Germany).

Confocal laser scanning microscopy

Laser scanning microscopy (LSM 510, Zeiss, Oberkochen, Germany) was performed to reveal co-localization of QC with TH, Ucn-1 and ChAT in LC, EWN and Nbm, respectively. For Cy2-labelled QC (green fluorescence), an argon laser with 488 nm excitation was used and emission from Cy2 was recorded at 510 nm applying a low-range band pass (505–550 nm). For Cy3-labelled TH, Ucn-1 and ChAT (red fluorescence), a helium-neon laser with 543 nm excitation was applied and emission from Cy3 at 570 nm was detected applying high-range band pass (560–615 nm).

Photoshop CS2 (Adobe Systems, Mountain View, CA, USA) was used to process the images obtained by light and confocal laser scanning microscopy with minimal alterations to brightness, sharpness, colour saturation and contrast.

Quantification of QC-immunoreactive neurons and pE-Aβ deposits

Quantitative analysis of ChAT-, Ucn-1-, TH- and QC-immunoreactive neurons and pE-Aβ deposits present in EWN, LC and human NbM was performed following the procedure described in [13]. Noradrenergic LC neurons in stained sections were additionally identified by the content of neuromelanin. Neurons were counted when the soma

and at least one dendrite could be identified. The outline of EWN, LC and NbM and the location of neurons inside these nuclei were assessed by means of a Stereoinvestigator (Microbrightfield, Williston, VT, USA; including a Zeiss Axioskop 2 plus, Märzhäuser micropositioning system and a Ludl 5000 controller) with the Neurolucida software. QC expression in EWN, LC and NbM was investigated in three sections from rostral to caudal (largely comprising the whole nucleus) in all cases. In sections analysed, the number of neurons labelled for the neuronal marker (e.g. ChAT, TH or Ucn-1) in each brain region of control brain was set to 100%. The relative numbers of QC-immunoreactive neurons and pE-Aβ deposits in brain regions analysed was calculated using the formula of Konigsmark [27].

Results

Distinct QC expression in the mouse EWN

First, QC immunohistochemistry was performed on mouse coronal midbrain sections at the level of bregma −3.1 to −3.8 mm. In the subcortical part of these sections, we only observed modest QC immunoreactivity in a relatively low percentage of neurons of some neuronal populations including substantia nigra and ventral tegmental area (not shown). In contrast, there was a small but robustly QC-expressing assembly of neurons within the EWN (Fig. 1). Labelling was absent from QC knock-out mouse brain sections, demonstrating the specificity of the immunohistochemical QC detection (Fig. 1). Since the EWN is known to be composed of a preganglionic cholinergic portion and a non-preganglionic, Ucn-1-positive part, we sought to identify the neuronal subpopulation expressing QC in this structure. Double immunofluorescent labellings revealed that QC is co-localised with Ucn-1 (Fig. 1) but not with ChAT (not shown) in neurons of the mouse EWN. Thus, QC-expressing neurons in the EWN represent the non-preganglionic, Ucn-1-positive part of this nucleus in mouse brain.

Distinct QC expression in the mouse locus coeruleus

In order to extend these findings and to substantiate a possible function of QC in pE-Aβ generation in vivo, we studied LC, a brainstem nucleus known to be severely affected in AD. As in the case of the EWN, there was strong and spatially defined QC labelling of neurons in the LC region of mouse brain (Fig. 2). This labelling was absent in brain sections from QC knock-out mice (Fig. 2). In order to clearly identify these neurons, immunofluorescent double labelling of QC and TH was performed. QC was found to be strictly co-localised to TH, demonstrating co-expression by mouse noradrenergic LC neurons (Fig. 2).

Distinct QC expression in the mouse nucleus basalis magnocellularis

In contrast to the robust QC expression by almost all mouse Ucn-1-positive EWN and TH-positive LC neurons, the mouse Nbm contained relatively few QC-immunoreactive neurons (Fig. 3). Double labelling with the cholinergic marker enzyme ChAT in this brain region revealed that approximately 50% of mouse Nbm cholinergic neurons co-expressed QC (Fig. 3).

It is important to note that in brains from QC knock-out mice, the neuronal marker proteins Ucn-1, TH and ChAT were detected in EWN, LC and Nbm neurons, respectively. This indicates survival of these neuronal populations in the absence of QC expression.

Distinct QC expression in human EWN, LC and NbM

We then asked whether QC is also expressed in the corresponding subcortical nuclei of human brain and whether pE-Aβ formation spatially correlates with QC expression in AD brains. Immunohistochemical labelling of human midbrain sections cut at the level of the EWN revealed a distinct and robust QC expression in this brain structure (Fig. 4), confirming observations made in mouse brain. In adjacent brain sections, two marker proteins of neuronal subpopulations of the EWN—Ucn-1 and ChAT—were visualised. In contrast to the mouse brain, the cholinergic part of this nucleus was much larger in relative size in human brain and contained more neurons when compared with the Ucn-1-positive portion (Fig. 4). Interestingly, QC expression was not limited to the Ucn-1-positive portion of the human EWN, but was also present in the cholinergic part of this brain structure (Fig. 4). This finding differs from the observations made in mice, where QC expression in the EWN was restricted to Ucn-1-positive neurons. Neurons in adjacent brain structures outside the EWN and perioculomotor area, such as red nucleus and superior colliculus did not display QC immunoreactivity.

Since we observed QC expression in mouse LC and because of the well-documented LC pathology in AD, we also examined human brainstem sections containing this structure. In similarity to observations made in mouse brain, QC was also found to be expressed by noradrenergic neurons in human LC (Fig. 4). The identity of QC-immunoreactive neurons as noradrenergic LC neurons was demonstrated by the typical neuronal pigment and by the expression of TH in consecutive brain sections. Interestingly, QC immunoreactivity was not limited to LC

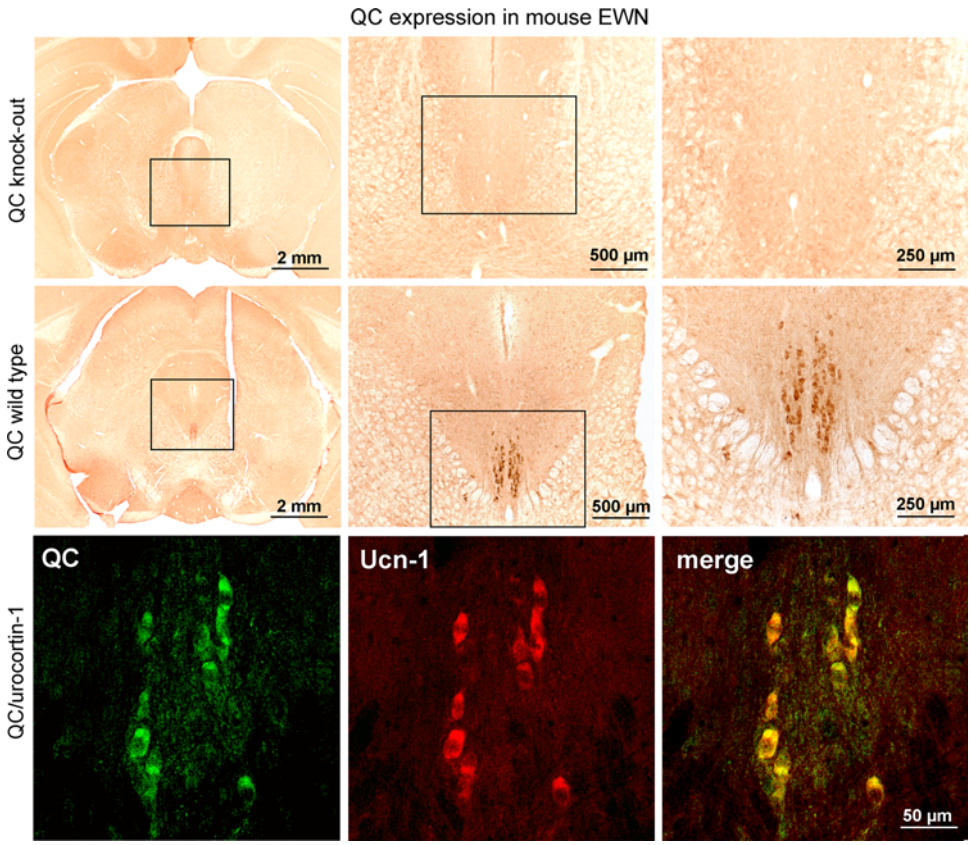

Fig. 1 QC expression in mouse Edinger–Westphal nucleus. *Top row* QC immunoreactivity is absent from midbrain sections of QC knock-out mice as shown at increasing magnifications from left to right. In contrast, there is a specific and robust labelling of a neuronal population in the EWN of wild type mice (*middle row*). Since the EWN is known to contain both, Ucn-1 and ChAT neurons, double labellings were performed. QC (green fluorescence) was found to be co-localised with Ucn-1 (red fluorescence; *bottom row*), but not with ChAT (not shown)

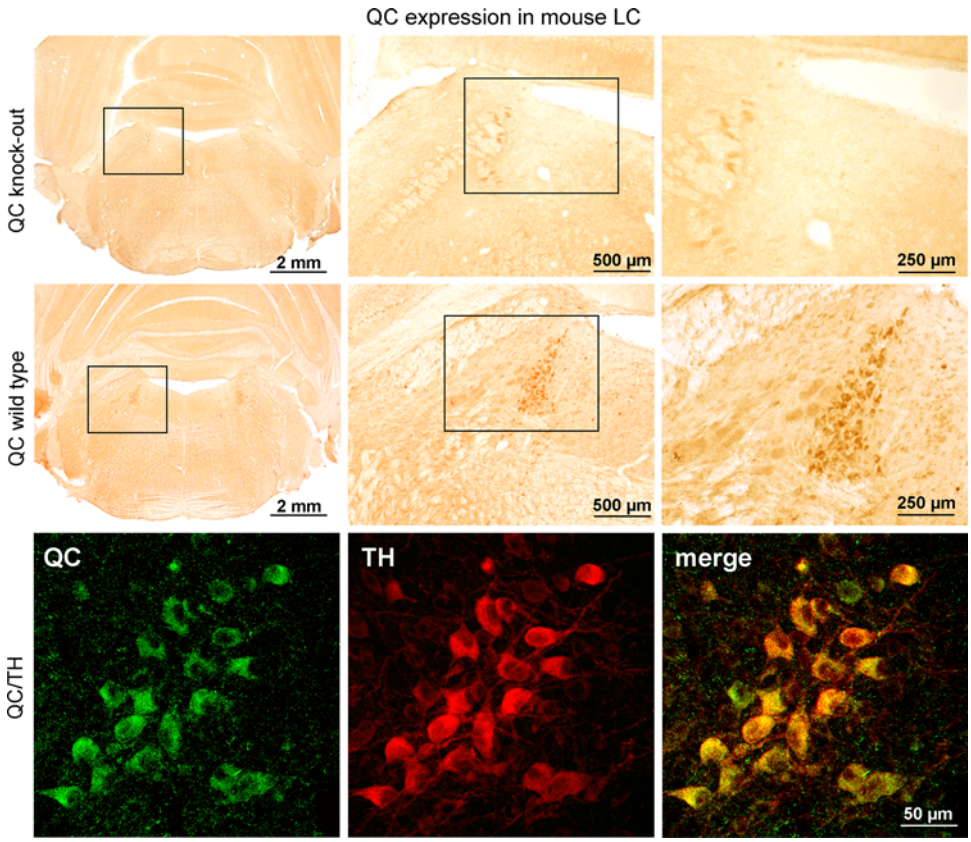

Fig. 2 QC expression in mouse locus coeruleus. *Top row* QC immunoreactivity is absent from brainstem sections of QC knock-out mice as shown at increasing magnifications from left to right. In contrast, there is a specific and robust QC labelling of a neuronal population corresponding to the LC of wild type mice (*middle row*). In order to identify these neurons as noradrenergic LC neurons, double labellings were performed. There was an almost complete overlap of QC (*green*) and TH (*red*) immunoreactivity in the mouse LC (*bottom row*)

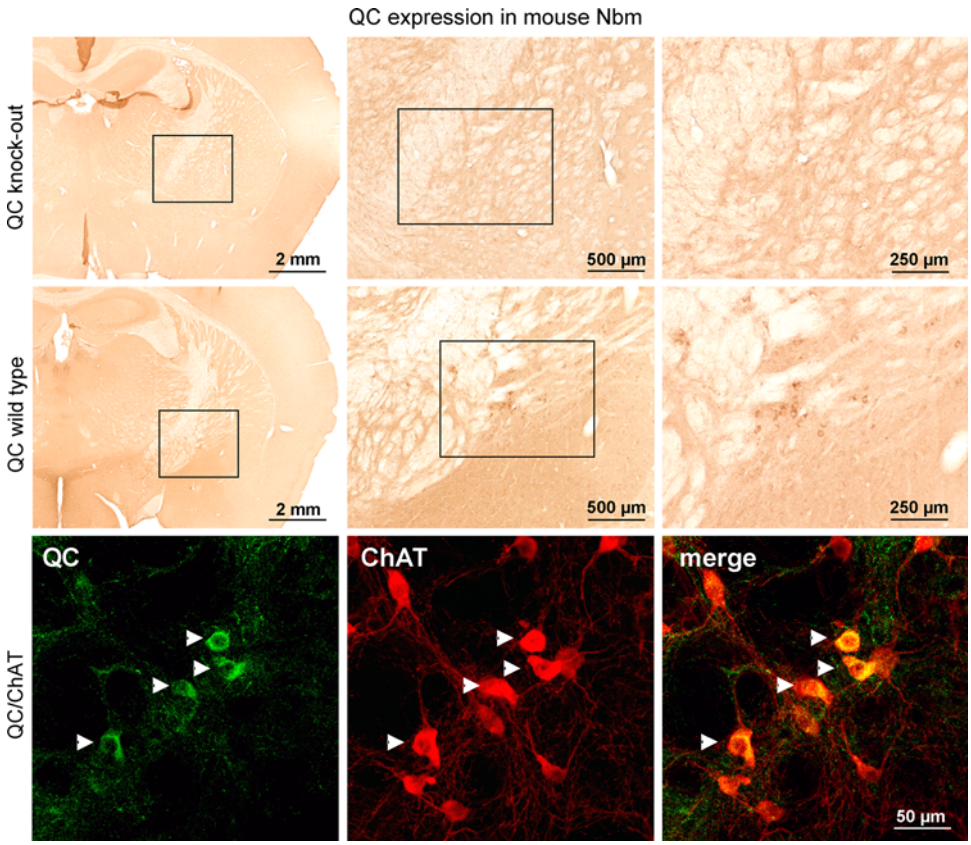

Fig. 3 QC expression in mouse nucleus basalis magnocellularis. *Top row* QC immunoreactivity is absent from basal forebrain sections of QC knock-out mice as shown at increasing magnifications from left to right. In contrast, there is a specific QC labelling of a neuronal population corresponding to the nucleus basalis of wild type mice (*middle row*). In order to identify these neurons as cholinergic basal forebrain neurons, double labellings were performed. QC (*green*) was found to be co-expressed by a proportion of ChAT-immunoreactive (*red*) neurons in the mouse nucleus basalis (*bottom row*). Double-labelled neurons are indicated by *yellow colour* in the overlay channel and by *arrows*

neuronal somata but was also detected in TH-positive fibres.

Although only a sub-population of cholinergic Nbm neurons in mouse brain contained QC, the analysis of human brain sections revealed strong QC expression by virtually all NbM neurons (Fig. 4). The intracellular pattern of QC immunoreactivity in the neuronal somata and processes was similar to that detected in EWN and LC.

Intraneuronal and extracellular pE-Aβ aggregates in the Alzheimer's disease EWN, LC and NbM

Given the high level of QC expression in human EWN, LC and NbM and the role of QC in pE-Aβ formation, we asked whether there is pE-Aβ plaque pathology in these human brain nuclei from AD patients. Using a mouse monoclonal antibody raised against pE-Aβ, we observed focal plaque formation in both, the Ucn-1-positive and the cholinergic portion of EWN as well as in LC and NbM of AD brain (Fig. 5). Similar to the QC staining pattern, brain structures outside the EWN and perioculomotor area, such as red nucleus and superior colliculus did not display pE-Aβ immunoreactivity. Additionally, we detected intraneuronal accumulation of pE-Aβ in EWN, LC and NbM neurons in brain tissue from AD patients but only rarely in normal brain (Fig. 5).

Quantitative analysis of QC expression and pE-Aβ deposit formation

In order to obtain quantitative data on the degree of QC expression and pE-Aβ deposit formation in the subcortical nuclei analysed, the numbers of Ucn-1 and cholinergic EWN, TH-positive LC and cholinergic NbM neurons were determined and the proportion of QC-positive neurons was calculated for each structure. In the normal human brain, almost all NbM neurons and approximately 80% of LC neurons co-expressed QC, whereas in the EWN only 20% of neurons were found to be QC immunoreactive (Fig. 6). In brains from AD patients, neuronal numbers were reduced by 39, 26 and 12% in NbM, LC and the Ucn-1 and cholinergic part of EWN, respectively (Fig. 6). Thus, the highest degree of neuronal loss was detected in the brain region with the most abundant QC expression. Additionally, a significant number of pE-Aβ deposits was detected in NbM, LC and EWN from AD patients but not from control subjects (Fig. 6). As in the case of neuronal loss, the most pronounced pE-Aβ deposit formation was observed in NbM of AD subjects.

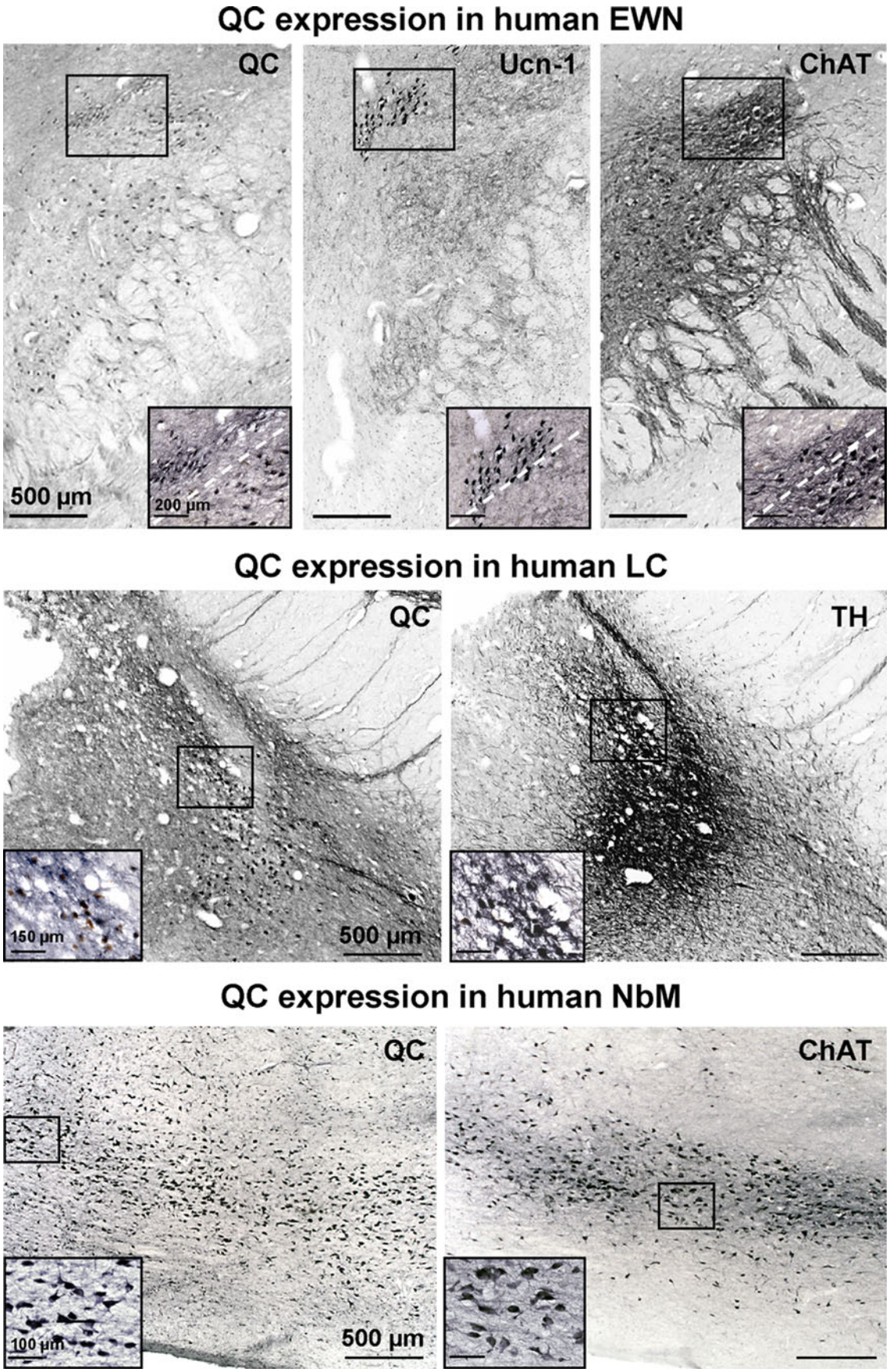
QC expression in human EWN
QC
Ucn-1
ChAT
500 µm
200 µm
QC expression in human LC
QC
TH
150 µm
500 µm
QC expression in human NbM
QC
ChAT
100 µm
500 µm

◀ **Fig. 4** QC expression in the human Edinger–Westphal nucleus, locus coeruleus and nucleus basalis Meynert. QC immunoreactivity was present in midbrain sections in a defined cell group (*top left*). These cells include both Ucn-1 and ChAT expressing subpopulations of the Edinger–Westphal nucleus as shown by the labelling of these marker proteins in adjacent brain sections. QC-immunoreactive neurons were also detected in brainstem sections in a small, defined cell group within the locus coeruleus area (*middle left*). Labelling of consecutive brain sections with TH identified these neurons as noradrenergic LC neurons (*middle right*). The highest density of QC-immunoreactive neurons was detected in the nucleus basalis Meynert (*bottom left*), which was identified by the presence of cholinergic Ch4 neurons (*bottom right*). *Scale bars* in overview 500 μm, in higher magnification inserts 100 μm, 150 μm and 200 μm as indicated

Discussion

The aim of this study was to reveal whether QC expression and pE-Aβ deposition can be spatially correlated with defined neuronal populations known to be affected by selective degeneration and by Aβ pathology in AD brains. For the initial screening of QC expression in the basal forebrain and brainstem, mice were used because of unrestricted access and the availability of QC knock-out mice as controls for the immunohistochemical QC labelling.

First, we demonstrated distinct QC expression by Ucn-1-positive EWN neurons in mice. Ucn-1 is a neuropeptide of the corticotropin-releasing factor (CRF) family and binds to CRF receptors 1 and 2, to the latter with higher affinity than CRF itself [65]. Ucn-1 is known to play a role in the regulation of food intake [63], energy balance [10] and anxiety [39] and Ucn-1 neurons of the EWN in particular appear to be involved in stress response [15, 28, 69] and alcohol consumption [3]. Interestingly, in a number of publications, midbrain structures including the EWN have been reported to display Aβ and Tau histopathology in AD patients [21, 45, 58, 59]. However, a comparison of these histological data appears difficult since the term EWN comprises several functionally different cell groups (preganglionic and several non-preganglionic cell groups, the latter including Ucn-1 positive neurons) and attempts have only been made recently to provide a clear and well-defined nomenclature of the EWN in mouse [68] and human brain [21, 22, 48].

With regard to QC expression in the EWN complex, we observed remarkable differences between mouse and human brain. Most strikingly, QC expression was limited to Ucn-1-positive EWN neurons in mice but also present in preganglionic cholinergic EWN neurons in humans. The

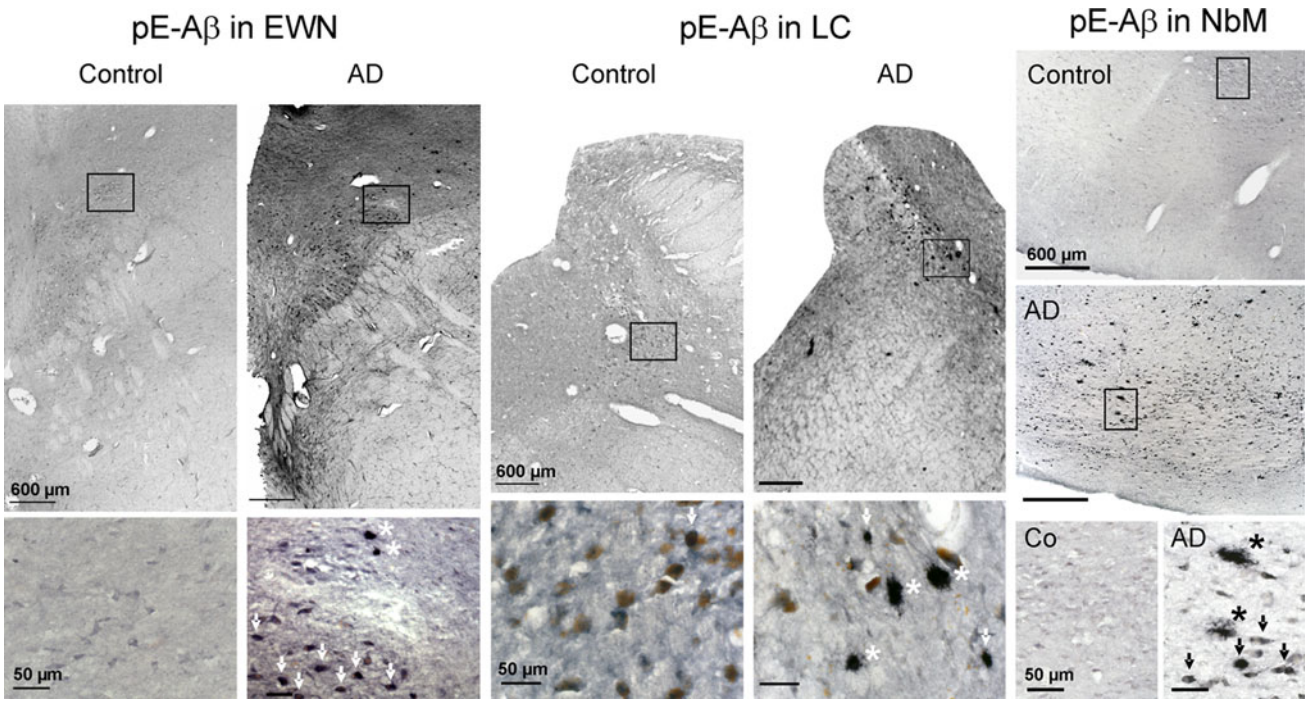

Fig. 5 pE-Aβ aggregates in human AD Edinger–Westphal nucleus, locus coeruleus and nucleus basalis Meynert. *Left* In the EWN of control subjects there was only a faint intraneuronal pE-Aβ immunoreactivity. In contrast, in brains from AD patients the EWN was robustly labelled with intraneuronal pE-Aβ (*arrows*) and pE-Aβ plaques (*asterisks*). *Middle* In the LC of control subjects numerous neurons containing neuropigment (*brown*) but rarely intraneuronal pE-Aβ accumulations (*arrow*) and no pE-Aβ deposits were present. In brains from AD patients there were intraneuronal pE-Aβ accumulations (*arrows*) and pE-Aβ immunoreactive plaques (*asterisks*). *Right* Intraneuronal pE-Aβ (*arrows*) and pE-Aβ deposits (*asterisks*) were detected in the NbM of AD patients but not in this brain region of control subjects. *Scale bars in top row* 600 μm, in *bottom row* 50 μm

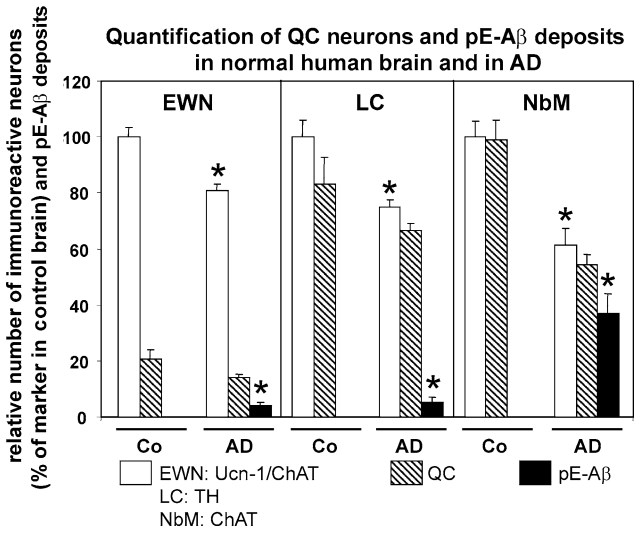

Fig. 6 Quantification of QC-expressing neurons and pE-Aβ deposits in normal human brain and in AD. The highest proportion of QC-immunoreactive neurons in control subjects was detected in the NbM, followed by LC and EWN. In all brain regions analysed, there was a reduction of the neuronal number in AD as identified by expression of Ucn-1/ChAT, TH and ChAT, respectively (* $p < 0.05$). While in control subjects no pE-Aβ deposits were detected in any of the brain nuclei investigated, a significant number of pE-Aβ deposits was detected in AD brains. Both, neuronal loss and formation of pE-Aβ deposits was most pronounced in NbM

latter neuronal population has a function in adaptive pupillary reaction, which has been reported to be affected in AD patients in response to treatment with cholinergic antagonists [57]. Our demonstration of QC expression, pE-Aβ formation and neurodegeneration in both Ucn-1 and cholinergic portions of EWN is in agreement with neuropathology in this nucleus observed earlier [45, 58, 59].

In addition to the EWN, we also demonstrated robust QC expression by a high proportion of noradrenergic LC neurons in mouse and human brain. LC degeneration is an early feature of AD pathology [14, 32]. The well-described noradrenergic neuronal loss [16] is accompanied by Aβ and Tau pathology and correlates with Aβ plaque load, neurofibrillary tangle formation and the severity of dementia [5, 6, 67, 71]. However, since LC neurons are known to provide essential noradrenergic innervation to the hippocampal formation and neocortex [30], it is conceivable that secondary morphological and neurochemical changes also occur in these target regions. Indeed, elevated hippocampal acetylcholine and serotonin release as observed in mild cognitive impairment patients was also detected after specific lesions of noradrenergic LC neurons in experimental animals [25]. Moreover, noradrenaline deficiency has been shown to promote neocortical and hippocampal Aβ pathology in transgenic animal models [20, 26]. Additionally, there is evidence for the seeding of neuritic Aβ plaques in target regions of brainstem neurons in AD [40].

This is also supported by the robust QC expression in human cholinergic NbM neurons. Interestingly, QC expression in the corresponding nucleus of mouse brain was less pronounced, a finding which might point towards a higher physiological relevance of QC expression in human NbM when compared with mouse Nbm neurons. In AD, the degeneration of cholinergic NbM neurons is an early and consistent pathological feature and results in cholinergic denervation of the cortical mantle [2, 9, 70]. This neocortical cholinergic hypoactivity has been correlated to the degree of dementia and is targeted by cholinomimetic approaches in order to at least temporarily attenuate cognitive decline in AD patients [44]. As in the case of noradrenergic LC neurons, cholinergic NbM neurons innervate brain regions severely affected by Aβ pathology and anterograde transport of QC and/or pE-Aβ may contribute to neocortical Aβ deposition. We thus believe that QC expression and subsequent pE-Aβ formation may play a causative role in the specific deterioration of cholinergic NbM and noradrenergic LC neurons and, subsequently, in the alteration of neocortical and hippocampal function and in the seeding of neuritic plaques in AD.

In all human brain regions with high QC expression studied here, we detected intraneuronal pE-Aβ and pE-Aβ plaques in the brains from AD patients. The monoclonal pE-Aβ antibody used in this study has been thoroughly characterised recently and was shown to detect pE-Aβ aggregates in neocortical brain tissue from sporadic and familial AD cases [73]. The pE-Aβ plaque load in NbM, LC and EWN was comparable to that reported for total Aβ deposits in these structures [2, 5, 45] and indicates that most, if not all, of these Aβ plaques contain pE-modified Aβ peptides. Interestingly, the proportion of QC-immunoreactive neurons and numbers of pE-Aβ deposits were highest in NbM, which also displayed the most profound neuronal loss in AD. In addition to the local formation of pE-Aβ aggregates at sites of QC-immunoreactive somata, pE-Aβ peptides may be released in target areas of projection neurons and may form Aβ plaques in brain regions devoid of QC and/or APP expression. Such a phenomenon was recently demonstrated in APP/PS1 knock-in mice with neocortical and hippocampal, but not thalamical, transgene expression [8]. The authors first observed intraneuronal Aβ in cortical neurons at 2 months of age, followed by extracellular cortical Aβ deposits at 6 months of age. In the thalamus of these mice, where no transgenic APP is expressed, extracellular Aβ deposits were detected at 6 months of age without preceding intracellular Aβ appearance. The authors concluded that Aβ may be deposited in brain regions where it is not produced via axonal transport and secretion from nerve terminals. Thus, in their animal model Aβ is produced in neocortex and

released from corticothalamic fibres in thalamus. In similarity to this scenario, our data suggest that pE-Aβ generated by EWN, LC and NbM neurons may be released at neocortical and hippocampal target regions.

Taken together, the demonstration of robust and spatially restricted QC expression and pE-Aβ formation in the EWN, LC and NbM provides further evidence for pE-Aβ formation by QC in vivo. Since pE-Aβ confers exceptional neurotoxicity [1, 47] and since intraneuronal pE-Aβ generation has been linked to neurodegeneration in animal models of AD [7, 72], QC-expressing EWN, LC and NbM neurons appear to be at high risk. Indeed, these neuronal populations are affected in AD and some clinical characteristics of AD patients such as dementia, anxiety, depression, compromised stress response and attention deficits [4, 9, 21, 35] could be—at least partially—attributed to compromised function of EWN, LC and NbM neurons. Moreover, in control subjects QC is expressed in all subcortical nuclei investigated without accompanying pE-Aβ deposit formation. This indicates a yet unidentified physiological function for QC outside the hypothalamus, which does not normally lead to pE-Aβ deposition or to neurodegeneration. In AD, however, there is pE-Aβ formation and neurodegeneration in LC, EWN and NbM. Thus, it appears that QC expression alone is not sufficient for pE-Aβ formation and neurotoxicity, but a dysbalance in the expression of APP, its processing by β- and γ-secretases and N-terminal Aβ truncation have to occur to generate the pathogenic QC substrate. In conclusion, we postulate that among multiple mechanisms contributing to the pathogenesis of AD, QC plays an important role in EWN, LC and NbM neurodegeneration and in pE-Aβ plaque pathology, both locally and in the cortical and hippocampal target regions of these projection neurons. As a consequence, pharmacological QC inhibition should reduce pE-Aβ production and exert beneficial effects on these neuronal populations.

Acknowledgments We thank R. Jendrek (Paul Flechsig Institute for Brain Research), H. Cynis, K. Schulz, M. Bornack, E. Scheel and M. Buchholz (Probiodrug) and S. Yu (Kinsmen Laboratory of Neurological Research) for technical assistance. This work was supported by the German Federal Department of Education, Science and Technology, BMBF grant #3013185 to HUD. Aspects of this work were also supported by the Pacific Alzheimer Research Foundation to CS and PLM and by the 7th Framework Program Health of the European Commission (Neuropro, Grant Agreement #223077) to SR. MM is member of the Graduiertenkolleg GRK 1097 funded by the German Research Foundation and of the MD/PhD program at the University of Leipzig.

Open Access This article is distributed under the terms of the Creative Commons Attribution Noncommercial License which permits any noncommercial use, distribution, and reproduction in any medium, provided the original author(s) and source are credited.

References

1. Acero G, Manutcharian K, Vasilevko V et al (2009) Immunodominant epitope and properties of pyroglutamate-modified Aβ-specific antibodies produced in rabbits. J Neuroimmunol 213:39–46
2. Arendt T, Bigl V, Tennstedt A, Arendt A (1985) Neuronal loss in different parts of the nucleus basalis is related to neuritic plaque formation in cortical target areas in Alzheimer's disease. Neuroscience 14:1–14
3. Bachtell RK, Weitemier AZ, Galvan-Rosas A et al (2003) The Edinger–Westphal-lateral septum urocortin pathway and its relationship to alcohol consumption. J Neurosci 23:2477–2487
4. Berridge CW, Waterhouse BD (2003) The locus coeruleus-noradrenergic system: modulation of behavioral state and state-dependent cognitive processes. Brain Res Rev 42:33–84
5. Bondareff W, Mountjoy CQ, Rossor RM, Iversen LL, Reynolds GP, Hauser DL (1987) Neuronal degeneration in the locus coeruleus and cortical correlates of Alzheimer's disease. Alzheimer Dis Assoc Disord 1:256–262
6. Busch C, Bohl J, Ohm TG (1997) Spatial, temporal and numeric analysis of Alzheimer changes in the nucleus coeruleus. Neurobiol Aging 18:401–406
7. Casas C, Sergeant N, Itier JM et al (2004) Massive CA1/2 neuronal loss with intraneuronal and N-terminal truncated Abeta42 accumulation in a novel Alzheimer transgenic model. Am J Pathol 165:1289–1300
8. Christensen DZ, Kraus SL, Flohr A, Cotel MC, Wirths O, Bayer TA (2008) Transient intraneuronal Aβ rather than extracellular plaque pathology correlates with neuron loss in the frontal cortex of APP/PS1 mice. Acta Neuropathol 116:647–655
9. Coyle JT, Price DL, DeLong MR (1983) Alzheimer's disease: a disorder of cortical cholinergic innervation. Science 219:1184–1190
10. Cullen MJ, Ling N, Foster AC, Pelleymounter MA (2001) Urocortin, corticotropin-releasing factor-2 receptors and energy balance. Endocrinology 142:992–999
11. Cynis H, Schilling S, Bodnar M et al (2006) Inhibition of glutaminyl cyclase alters pyroglutamate formation in mammalian cells. Biochim Biophys Acta 1764:1618–1625
12. D'Arrigo C, Tabaton M, Perico A (2009) N-terminal truncated pyroglutamyl beta amyloid peptide Abetapy3–42 shows a faster aggregation kinetics than the full-length Abeta1–42. Biopolymers 91:861–873
13. Damier P, Hirsch EC, Agid Y, Graybiel AM (1999) The substantia nigra of the human brain. I. Nigrosomes and the nigral matrix, a compartmental organization based on calbindin D28K immunohistochemistry. Brain 122:1421–1436
14. Forno LS (1978) The Locus coeruleus in Alzheimer's disease. J Neuropath Exp Neurol 37:614
15. Gaszner B, Jensen KO, Farkas J et al (2009) Effects of maternal separation on dynamics of urocortin 1 and brain-derived neurotrophic factor in the rat non-preganglionic Edinger–Westphal nucleus. Int J Dev Neurosci 27:439–451
16. German DC, Manaye KF, White CL III et al (1992) Disease-specific patterns of locus coeruleus cell loss. Ann Neurol 32:667–676
17. Hardy JA, Higgins GA (1992) Alzheimer's disease: the amyloid cascade hypothesis. Science 256:184–185
18. Hartlage-Rübsamen M, Staffa K, Waniek A et al (2009) Developmental expression and subcellular localization of glutaminyl cyclase in mouse brain. Int J Dev Neurosci 27:825–835
19. He W, Barrow CJ (1999) The A beta 3-pyroglutamyl and 11-pyroglutamyl peptides found in senile plaque have greater beta-

sheet forming and aggregation propensities in vitro than full-length A beta. Biochemistry 38:10871–10877
20. Heneka MT, Ramanathan M, Jacobs AH et al (2006) Locus coeruleus degeneration promotes Alzheimer pathogenesis in amyloid precursor protein 23 transgenic mice. J Neurosci 26:1343–1354
21. Horn AK, Eberhorn A, Härtig W, Ardeleanu P, Messoudi A, Büttner-Ennever JA (2008) Perioculomotor cell groups in monkey and man defined by their histochemical and functional properties: reappraisal of the Edinger–Westphal nucleus. J Comp Neurol 507:1317–1335
22. Horn AK, Schulze C, Radtke-Schuller S (2009) The Edinger–Westphal nucleus represents different functional cell groups in different species. Ann N Y Acad Sci 1164:45–50
23. Iwatsubo T, Odaka A, Suzuki N, Mizusawa H, Nukina N, Ihara Y (1994) Visualization of Abeta 42(43) and Abeta 40 in senile plaques with end-specific Abeta monoclonals: evidence that an initially deposited species is Abeta 42(43). Neuron 13:45–53
24. Iwatsubo T, Mann DM, Odaka A, Suzuki N, Ihara Y (1995) Amyloid beta protein (Abeta) deposition: Abeta 42(43) precedes Abeta 40 in Down syndrome. Ann Neurol 37:294–299
25. Jackisch R, Gansser S, Cassel JC (2008) Noradrenergic denervation facilitates the release of acetylcholine and serotonin in the hippocampus: towards a mechanism underlying upregulations described in MCI patients? Exp Neurol 213:345–353
26. Kalinin S, Gavrilyuk V, Polak P et al (2007) Noradrenaline deficiency in brain increases β-amyloid plaque burden in an animal model of Alzheimer's disease. Neurobiol Aging 28:1206–1214
27. Konigsmark BW (1970) Methods for the counting of neurons. In: Nauta WHJ, Ebbesson SOE (eds) Contemporary research methods in neuroanatomy. Springer, Berlin, pp 315–380
28. Koob GF, Heinrichs SC (1999) A role of corticotropin-releasing factor and urocortin in behavioral responses to stressors. Brain Res 848:141–152
29. Liu K, Solano I, Mann D et al (2006) Characterization of Abeta11–40/42 peptide deposition in Alzheimer's disease and young Down's syndrome brains: implication of N-terminally truncated Abeta species in the pathogenesis of Alzheimer's disease. Acta Neuropathol 112:163–174
30. Loy R, Koziell DA, Lindsay JD, Moore RY (1980) Noradrenergic innervation of the adult rat hippocampal formation. J Comp Neurol 189:699–710
31. Mai JK, Assheuer J, Paxinos G (2004) Atlas of the human brain. Academic Press, San Diego
32. Mann DM, Yates PO, Marcyniuk B (1984) Monoaminergic neurotransmitter systems in presenile Alzheimer's disease and in senile dementia of Alzheimer type. Clin Neuropathol 3:199–205
33. Marcyniuk NB, Mann DM, Yates PO (1986) The topography of cell loss from locus coeruleus in Alzheimer's disease. J Neurol Sci 76:335–345
34. Marcyniuk NB, Mann DM, Yates PO (1986) Loss of nerve cells from locus coeruleus in Alzheimer's disease is topographically arranged. Neurosci Lett 64:247–252
35. Marino MD, Bourdelat-Parks BN, Weinshenker D (2005) Genetic reduction of noradrenergic function alters social memory and reduces aggression in mice. Behav Brain Res 161:197–208
36. McColl G, Roberts BR, Gunn AP et al (2009) The *Caenorhabditis elegans* Aβ1-42 model of Alzheimer's disease predominantly expresses Aβ3-42. J Biol Chem 284:22697–22702
37. McKhann G, Drachmann D, Folstein M, Katzman R, Price D, Stadlan EM (1984) Clinical diagnosis of Alzheimer's disease: report of the NINCDS-ADRDA work group under the auspices of Department of Health and Human Services Task Force on Alzheimer's disease. Neurology 34:939–944
38. Miravalle L, Calero M, Takao M, Roher AE, Ghetti B, Vidal R (2005) Amino-terminally truncated Abeta peptide species are the main component of cotton wool plaques. Biochemistry 44:10810–10821
39. Moreau JL, Kilpatrick G, Jenck F (1997) Urocortin, a novel neuropeptide with anxiogenic-like properties. Neuroreport 8:1697–1701
40. Muresan Z, Muresan V (2008) Seeding neuritic plaques from the distance: a possible role for brainstem neurons in the development of Alzheimer's disease. Neurodegener Dis 5:250–253
41. Paxinos G, Huang XF, Toga AW (2000) The rhesus monkey brain in stereotaxic coordinates. Academic Press, San Diego
42. Paxinos G, Huang XF (1995) Atlas of the human brainstem. Academic Press, San Diego
43. Piccini A, Russo C, Gliozzi A et al (2005) Beta-amyloid is different in normal aging and in Alzheimer's disease. J Biol Chem 280:34186–34192
44. Roßner S, Ueberham U, Schliebs R, Perez-Polo JR, Bigl V (1998) The regulation of amyloid precursor protein metabolism by cholinergic mechanisms and neurotrophin receptor signaling. Prog Neurobiol 56:541–569
45. Rüb U, Del Tredici K, Schultz C, Büttner-Ennever JA, Braak H (2001) The premotor region essential for rapid vertical eye movements shows early involvement in Alzheimer's disease-related cytoskeletal pathology. Vision Res 41:2149–2156
46. Russo C, Schettini G, Saido TC et al (2000) Presenilin-1 mutations in Alzheimer's disease. Nature 405:531–532
47. Russo C, Violani E, Salis S et al (2002) Pyroglutamate-modified amyloid beta-peptides–AbetaN3(pE)–strongly affect cultured neuron and astrocyte survival. J Neurochem 82:1480–1489
48. Ryabinin AE, Tsivkovskaia NO, Ryabinin SA (2005) Urocortin 1-containing neurons in the human Edinger–Westphal nucleus. Neuroscience 134:1317–1323
49. Saido TC (1998) Alzheimer's disease as proteolytic disorders: anabolism and catabolism of beta-amyloid. Neurobiol Aging 19:S69–S75
50. Saido TC, Iwatsubo T, Mann DM, Shimada H, Ihara Y, Kawashima S (1995) Dominant and differential deposition of distinct beta-amyloid peptide species, Abeta N3(pE), in senile plaques. Neuron 14:457–466
51. Saido TC, Yamao H, Iwatsubo T, Kawashima S (1996) Amino- and carboxyl-terminal heterogeneity of beta-amyloid peptides deposited in human brain. Neurosci Lett 215:173–176
52. Schilling S, Hoffmann T, Manhart S, Hoffmann M, Demuth HU (2004) Glutaminyl cyclases unfold glutamyl cyclase activity under mild acid conditions. FEBS Lett 563:191–196
53. Schilling S, Lauber T, Schaupp M et al (2006) On the seeding and oligomerization of pGlu-amyloid peptides (in vitro). Biochemistry 45:12393–12399
54. Schilling S, Zeitschel U, Hoffmann T et al (2008) Glutaminyl cyclase inhibition attenuates pyroglutamate Abeta and Alzheimer's disease-like pathology. Nat Med 14:1106–1111
55. Schilling S, Appl T, Hoffmann T et al (2008) Inhibition of glutaminyl cyclase prevents pGlu-Aβ formation after intracortical/hippocampal microinjection in vivo/in situ. J Neurochem 106:1225–1236
56. Schlenzig D, Manhart S, Cinar Y et al (2009) Pyroglutamate formation influences solubility and amyloidogenicity of amyloid peptides. Biochemistry 48:7072–7078
57. Scinto LF, Daffner KR, Dressler D et al (1994) A potential noninvasive neurobiological test for Alzheimer's disease. Science 266:1051–1054
58. Scinto LF, Wu CK, Firla KM, Daffner KR, Saroff D, Geula C (1999) Focal pathology in Edinger–Westphal nucleus explains pupillary hypersensitivity in Alzheimer's disease. Acta Neuropathol 97:557–564

59. Scinto LF, Frosch M, Wu CK, Daffner KR, Gedi N, Geula C (2001) Selective cell loss in Edinger–Westphal in asymptotic elders and Alzheimer's patients. Neurobiol Aging 22:729–736
60. Selkoe DJ, Schenk D (2003) Alzheimer's disease: molecular understanding predicts amyloid based therapeutics. Annu Rev Pharmacol Toxicol 43:545–584
61. Sergeant N, Bombois S, Ghestem A et al (2003) Truncated beta-amyloid peptide species in pre-clinical Alzheimer's disease as new targets for the vaccination approach. J Neurochem 85:1581–1591
62. Shin RW, Ogino K, Kondo A et al (1997) Amyloid beta-protein (Abeta) 1–40 but not Abeta1-42 contributes to the experimental formation of Alzheimer disease amyloid fibrils in rat brain. J Neurosci 17:8187–8193
63. Spina M, Merlo-Pich E, Chan RK et al (1996) Appetite-suppressing effects of urocortin, a CRF-related neuropeptide. Science 273:1561–1564
64. Vanderstichele H, De Meyer G, Andreasen N et al (2005) Amino-truncated {beta}-amyloid42 peptides in cerebrospinal fluid and prediction of progression of mild cognitive impairment. Clin Chem 51:1650–1660
65. Vaughan J, Donaldson C, Bittencourt J et al (1995) Urocortin, a mammalian neuropeptide related to fish urotensin I and to corticotropin-releasing factor. Nature 378:287–292
66. Vida I, Halasy K, Szinyei C, Somogyi P, Buhl EH (1998) Unitary IPSPs evoked by interneurons at the stratum radiatum-stratum lacunosum-moleculare border in the CA1 area of the rat hippocampus in vitro. J Physiol 506:755–773
67. Weinshenker D (2008) Functional consequences of locus coeruleus degeneration in Alzheimer's disease. Curr Alzheimer Res 5:342–345
68. Weitemier AZ, Tsivkovskaia NO, Ryabinin AE (2005) Urocortin 1 distribution in mouse brain is strain-dependent. Neuroscience 132:729–740
69. Weninger SC, Peters LL, Majzoub JA (2000) Urocortin expression in the Edinger–Westphal nucleus is up-regulated by stress and corticotropin-releasing hormone deficiency. Endocrinology 141:256–263
70. Whitehouse PJ, Price DL, Clark AW, Coyle JT, DeLong MR (1981) Alzheimer's disease: evidence for selective loss of cholinergic neurons in the nucleus basalis. Ann Neurol 10:122–126
71. Wilcock GK, Esiri MM, Bowen DM, Hughes AO (1988) The different involvement of subcortical nuclei in senile dementia of Alzheimer's type. J Neurol Neurosurg Psychiatry 51:842–849
72. Wirths O, Breyhan H, Cynis H, Schilling S, Demuth HU, Bayer TA (2009) Intraneuronal pyroglutamate-Abeta 3–42 triggers neurodegeneration and lethal neurological deficits in a transgenic mouse model. Acta Neuropathol 118:487–496
73. Wirths O, Bethge T, Marcello A et al (2010) Pyroglutamate Abeta pathology in APP/PS1KI mice, sporadic and familial Alzheimer's disease. J Neural Transm 117:85–96